Determination of H^N,H_α and H^N,C' coupling constants in $^{13}C,^{15}N$-labeled proteins

R. Weisemann[a], H. Rüterjans[a],
H. Schwalbe[b], J. Schleucher[b], W. Bermel[c] and C. Griesinger[b,*]

[a]Institut für Biophysikalische Chemie and [b]Institut für Organische Chemie, Universität Frankfurt, Marie-Curie-Strasse 11,
D-60439 Frankfurt, Germany
[c]Bruker Analytische Meßtechnik GmbH, Silberstreifen, D-76287 Rheinstetten, Germany

SUMMARY

Sensitive three-dimensional NMR experiments, based on the E.COSY principle, are presented for the measurement of the $^3J(H^N,H_\alpha)$ and $^3J(H^N,C')$ coupling constants in uniformly ^{13}C- and ^{15}N-labeled proteins. They employ gradient coherence selection in combination with the sensitivity enhancement method in HSQC-type spectra (Cavanagh et al., 1991; Palmer et al., 1991). In most cases, the two measured coupling constants unambiguously define the φ-angle for protein structure determination. The method is applied to uniformly $^{13}C,^{15}N$-labeled ribonuclease T_1.

INTRODUCTION

The φ-angle in proteins can be determined from $^3J(H^N,H_\alpha)$ and $^3J(H^N,C')$ coupling constants. In this paper we present a new method for the measurement of $^3J(H^N,C')$. This method and an improved version of the recently proposed method for the measurement of $^3J(H^N,H_\alpha)$ coupling constants (Sørensen, 1990; Wagner et al., 1991; Seip et al., 1992; Madsen et al., 1993) both rely on the well-established E.COSY principle (Sørensen, 1984; Griesinger et al. 1985, 1986, 1987) to measure small coupling constants. The incorporation of sensitivity enhancement (Cavanagh et al., 1991; Palmer et al., 1991) in conjunction with the use of a heteronuclear gradient echo (Kay et al., 1992; Muhandiram et al., 1993; Schleucher et al., 1993) in the sensitivity-enhanced $N \rightarrow H^N$ transfer part of the HNCA sequence provides optimal water suppression, together with high sensitivity.

A single coupling constant does not unambiguously define a dihedral angle, since the Karplus

---

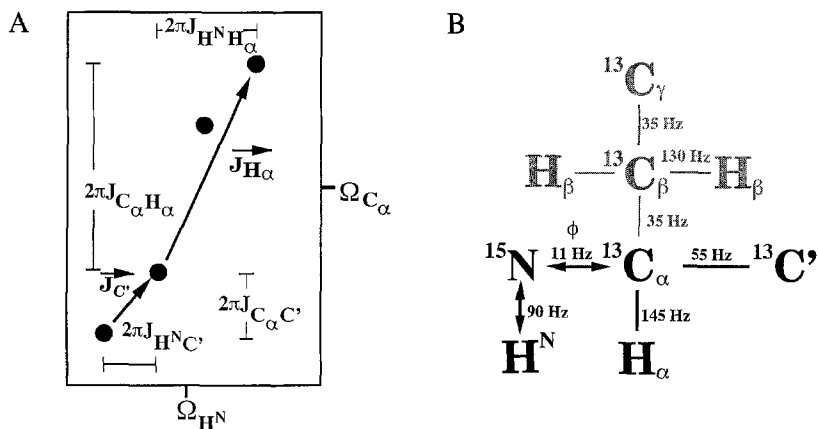*To whom correspondence should be addressed.

Fig. 1. (A) Schematic multiplet pattern obtained in a correlation of C_α and NH without decoupling of the couplings to C' and H_α. The displacement vectors $\vec{J}_{H_\alpha}$ and $\vec{J}_{C'}$ with their components are indicated. Two experiments that are either C'- or H_α-decoupled yield the $^3J(H^N,H_\alpha)$ or $^3J(H^N,C')$ couplings, respectively. (B) The correlated atoms in the HNCA-COSY experiments.

relation is up to fourfold degenerate. The measurement of two coupling constants about the backbone angle ϕ allows to resolve this ambiguity if ϕ assumes one value (see Fig. 1A). The novel pulse sequences for the determination of $^3J(H^N,H_\alpha)$ and $^3J(H^N,C')$ are applied to ribonuclease T_1, containing 104 amino acids.

METHODS

$^3J(H^N,H_\alpha)$ and $^3J(H^N,C')$ coupling constants can be measured in an E.COSY-type fashion by the correlation of C_α with H^N, using either H_α or C' as the passive spin in an experiment derived from HNCA (Ikura et al., 1990; Kay et al., 1990; Farmer II et al., 1992; Grzesiek and Bax, 1992). The schematic multiplet pattern, the nuclei and the ^1J coupling constants used for coherence transfer are shown in Fig. 1B. The experiment directed to the measurement of $^3J(H^N,H_\alpha)$ couplings is an extension of the experiment proposed by Seip et al. (1992), using sensitivity-enhanced gradient selection of the coherence transfer pathway, and will be called Soft HNCA-E.COSY (for pulse sequences see Fig. 2A,D), since sensitivity enhancement is combined in a HNCA sequence using H_α as passive spin. The coupling constants obtained by the non-gradient and the gradient version of the experiment will be compared.

The usage of C' as passive spin in E.COSY-type experiments with the $^1J(C_\alpha,C')$ of 55 Hz as associated coupling has been used in a number of applications (Eggenberger et al., 1992a; Vuister and Bax, 1992; Schwalbe et al., 1993). Leaving C' passive in the HNCA experiment yields the $^3J(H^N,C')$ coupling constant. Again, this experiment can be run in a gradient as well as a non-gradient version (Fig. 2B,E).

Both couplings could be measured in a combined experiment. (Fig. 2C), in which both H_α and C' are simultaneously used as passive spins. However, the combined spectrum has a sensitivity that is a factor of $\sqrt{2}$ lower, compared to recording two separate experiments (Eggenberger et al., 1992a).

Measurement of $^3J(H^N,H_\alpha)$: Soft HNCA-E.COSY or gradient sensitivity-enhanced Soft HNCA-E.COSY

The pulse sequence (Fig. 2A,D) used to measure the $^3J(H^N,H_\alpha)$ coupling constants is the sequence originally published by Seip et al. (1992), improved by the use of a heteronuclear gradient echo combined with sensitivity enhancement in the $N \rightarrow H^N$ INEPT step and a constant time evolution during the magnetization transfer step from C_α to ^{15}N. The use of heteronuclear gradient echos (Kay et al., 1992; Muhandiram et al., 1993; Schleucher et al., 1993) in conjunction with sensitivity enhancement has been shown to yield optimal sensitivity and water suppression. The idea behind this is to record a spectrum which is phase-modulated in t_1, rather than amplitude-modulated.

Combining amplitude-modulating experiments with gradient selection of coherence pathways inherently leads to a loss in S/N of a factor $\sqrt{2}$, since only one of two possible coherence pathways can be selected in the evolution time of the heteronuclei. In phase-modulating experiments only one coherence order contributes to the signal during the evolution time. This signal can therefore be selected by the formation of a heteronuclear gradient echo without loss in sensitivity as shown for various multidimensional experiments (Kay et al., 1992; Muhandiram et al., 1993; Schleucher et al., 1993). Therefore these experiments have a sensitivity of a factor 2 larger than that obtained by incorporation of a heteronuclear gradient echo in the corresponding amplitude-modulating sequence. The heteronuclear gradient echo is generated by application of a gradient pulse with strength $2\tau_g \cdot 5G_z$ during ^{15}N chemical shift evolution, combined with a gradient with strength $\pm \tau_g \cdot G_z$ prior to acquisition (τ_g is the duration of the gradient pulse). In combination with the phase $\psi = \pm y$ of the last ^{15}N 90° pulse in the sequence, this results in echo ($N_- \rightarrow H_-$) and antiecho ($N_+ \rightarrow H_-$) selection, respectively. The unusual coherence transfers of echo and antiecho are due to negative gyromagnetic ratio of ^{15}N. The echo and antiecho FIDs are stored separately. From this data a complex data set is generated in a format according to States et al. (1984). The sum of the two FIDs is used as the real part and the difference after a 90° phase correction as the imaginary part of the signal in the ^{15}N evolution period. Application of the heteronuclear gradient echo requires the ^{15}N chemical shift to evolve towards the end of the pulse sequence, in order not to lose sensitivity due to diffusion effects.

The compatibility of the sensitivity-enhanced reverse INEPT (Cavanagh et al., 1991; Palmer et al., 1991) with the requirement not to disturb the H_α from the beginning of t_1 to the end of t_3 has been demonstrated by Madsen et al. (1993). Considering only the large ^1J coupling constants and chemical shifts, the chemical shift of the H_α and the heteronuclear coupling of the H_α to the C_α are refocussed in each delay during the $N \rightarrow H^N$ transfer. Then the proton pulse train 90°_x-180°_y-90°_y-180°_y-90°_x-180°_x in the sensitivity enhanced $N \rightarrow H^N$ transfer part can be concatenated, which leads to a 360°_x pulse for z-magnetization of H_α, which fulfills the E.COSY requirement.

However, it has not been analysed whether the evolution of homonuclear and heteronuclear long-range couplings can be neglected in the sensitivity-enhanced $N \rightarrow H^N$ transfer. The two operators present at the start of the $N \rightarrow H^N$ transfer step, $2N^\pm(H^N)_z(H_\alpha)^\alpha$ and $2N^\pm(H^N)_z(H_\alpha)^\beta$, evolve differently during the last part of the pulse sequence, possibly giving rise to systematic errors in the determination of the $^3J(H^N,H_\alpha)$ coupling. $((H_\alpha)^\alpha, (H_\alpha)^\beta$ represent the α-proton in spin state α or β.) In order to investigate this systematic error, which is equivalent to the undesired correlation of nonconnected transitions in an E.COSY-type experiment, a series of 1D spectra was simulated with an initial state of the density matrix corresponding to an antiphase operator
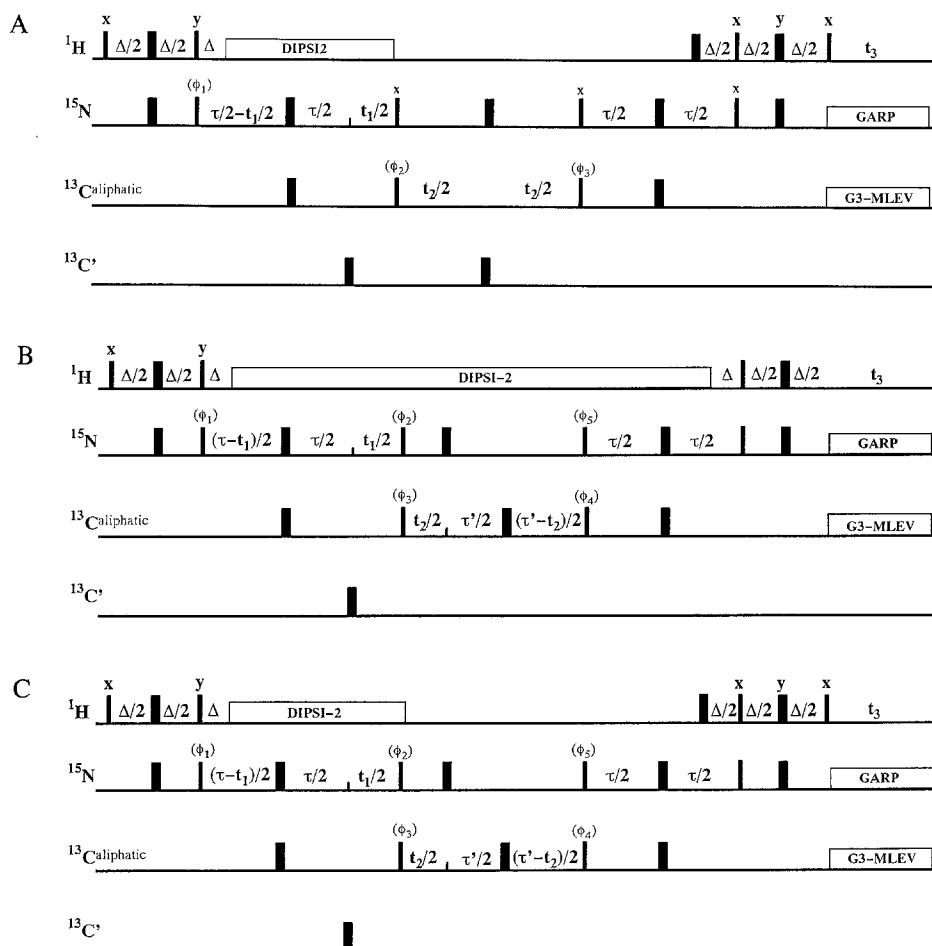
234

Fig. 2. Pulse sequences for the experiments. (A) Soft CT-HNCA-E.COSY. Eight scans per t_1 (64 experiments, $t_1^{max} = 16\,ms$), t_2 (256 experiments, $t_2^{max} = 25.6\,ms$) experiment were recorded with 512 complex points in t_3 (spectral width 4504 Hz). H_2O was saturated using off-resonance irradiation for 1.5 s and a high-power trim pulse (Messerle et al., 1989) of 2 ms was applied before the second ^1H 90° pulse along x (not shown in the pulse sequence). The experiment was carried out on a Bruker AMX 600 spectrometer, equipped with a triple-resonance inverse $^1H,^{13}C,^{15}N$ probe. The delays were set as follows: $\Delta = 5.36\,ms$, $\Delta' = 2.5\,ms$, $\tau = 41.6\,ms$, $\tau' = 28.57\,ms$. Every second G4 (Gaussian Cascade Inversion Pulse, introduced by Emsley and Bodenhausen, 1989, 1990) pulse was time-reversed in order to avoid accumulation of phase errors from successive G4 pulses. Carbonyl-selective 180° pulses were implemented as phase-modulated G3 pulses of 256 μs length. Protons were decoupled during $\tau - \Delta$ using the DIPSI-2 (Shaka, 1988) decoupling sequence with a field strength $\gamma B_1/2\pi$ of 3.1 kHz. Zero-order Bloch–Siegert shift of C_α due to the off-resonance carbonyl pulse in the middle of t_2 was compensated for by correction of the phase of the ^{13}C 90° pulse before t_2. ^{15}N was decoupled using a GARP decoupling sequence (Shaka, 1983) with a field strength of 1.1 kHz. Simultaneous decoupling of aliphatic and carbonyl carbons was performed using amplitude-modulated G3 pulses of 512 μs length, expanded according to MLEV-16 (Levitt et al., 1982) and MLEV-8 (Eggenberger et al., 1992b). States-TPPI (Bax et al., 1991) on the first ^{15}N 90° pulse and on the ^{13}C 90° pulse was used for frequency sign discrimination in t_1 and t_2. The pulses for which phases are not explicitly given were applied along the x-axis. $\phi_1 = x,-x$; $\phi_2 = 2x,2(-x)$; $\phi_3 = 4x,4(-x)$; Rec. $= \Sigma\,\phi_i = x,-x,-x,\,x,-x,\,x,\,x,-x$. (B) Soft HNCA-COSY. The same parameters as in (A) have been used except for: Eight scans per t_1 (64 experiments, $t_1^{max} = 16\,ms$), t_2 (280 experiments, $t_1^{max} = 28.57\,ms$) experiment were recorded with 512 complex points in t_3 (spectral width 5000 Hz). Protons were decoupled
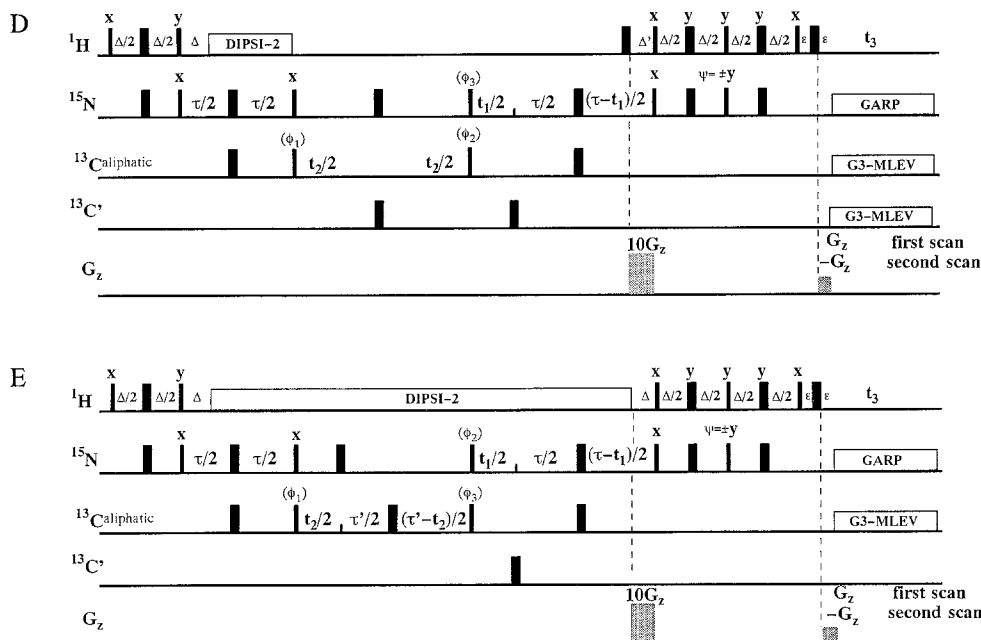
during $2\tau + \tau' - 2\Delta$. Aliphatic carbon decoupling was achieved with an MLEV-16 expansion of G3 pulses of 512 µs length. The phase cycling was identical to that in (A). (C) Combined Soft HNCA-COSY. The experiment has been run as a two-dimensional version, recording the first ω_2,ω_3-slice of the 3D experiment. 128 scans (280 experiments, $t_2^{max} = 28.57$ ms) were recorded with 512 complex points in t_3. The pulses for which phases are not explicitly given were applied along the x-axis. $\phi_1 = x,-x$; $\phi_2 = 2x,2(-x)$; $\phi_3 = 4x,4(-x)$; $\phi_4 = 8x,8(-x)$; Rec. $= \Sigma \phi_i$. (D) Gradient sensitivity enhanced Soft HNCA-E.COSY. Eight scans per t_1 (48 experiments, $t_1^{max} = 12$ ms), t_2 (128 experiments, $t_2^{max} = 12.8$ ms) experiment were recorded with 512 complex points in t_3 (spectral width 4504 Hz). The experiment was recorded on a Bruker AMX 600 spectrometer, equipped with a gradient triple-resonance $^1H,^{13}C$ broadband probe. The delays were set as follows: $\Delta = 5.5$ ms, $\Delta = 2.5$ ms, $\tau = 26$ ms, $\tau' = 27$ ms, $\varepsilon = 2.39$ ms. A high-power trim pulse of 2 ms was applied before the second ^1H 90° pulse along the x-axis (not shown in the pulse sequence). Gradients for coherence selection were applied with a maximum field strength of 45 G/cm and durations of 4.3 and 2 ms (200 µs recovery). For practical reasons the gradient 10 G_z during the ^{15}N evolution time was applied during $\tau/2$ instead of Δ'. The sign of the second gradient was inverted, together with the phase of the last ^{15}N 90° pulse. G3 and G4 pulses had durations of 256 and 409.6 µs, respectively. Every second G4 pulse was again time-reversed. Carbonyl-selective pulses were implemented as phase-modulated G3 pulses of 256 µs duration. Protons were decoupled during $\tau - \Delta$. Zero-order Bloch–Siegert shift on C_α due to the off-resonance carbonyl pulse in the middle of t_2 was compensated for by adjusting the phase of the ^{13}C 90° pulse before t_2. Simultaneous decoupling of aliphatic and carbonyl was done with an MLEV-16 expansion of double phase-modulated G3 pulses of 512 µs length. ^{15}N was decoupled using a GARP decoupling sequence (Shaka et al., 1985) with a field strength of 1.1 kHz. States-TPPI on the ^{13}C 90° pulse before the t_2 period was used for frequency sign discrimination in t_2. Sign discrimination in t_1 was achieved by storing every alternating scan for $\psi = \pm y$ separately. The two FIDs are added and subtracted, and for the resulting subtracted FID real and imaginary data are swapped. This subtracted and swapped FID is stored as imaginary part, whereas the added FID is stored as the real part of the signal in t_1 (see text for further explanation). The pulses for which phases are not explicitly given were applied along the x-axis. $\phi_1 = x,-x$; $\phi_2 = 2x,2(-x)$; $\phi_3 = 4x,4(-x)$; Rec. $= \Sigma \phi_i$. (E) Gradient sensitivity-enhanced Soft HNCA-COSY. The same parameters as in (D) have been used except for: Eight scans per t_1 (64 experiments, $t_1^{max} = 16$ ms), t_2 (264 experiments, $t_2^{max} = 27$ ms) experiment were recorded with 512 complex points in t_3 (spectral width 4504 Hz). Protons were decoupled during $2\tau' + \tau - 2\Delta$ using the DIPSI-2 decoupling sequence with a field strength of 4 kHz. Aliphatic carbon decoupling was achieved with an MLEV-16 expansion of G3 pulses of 512 µs duration.
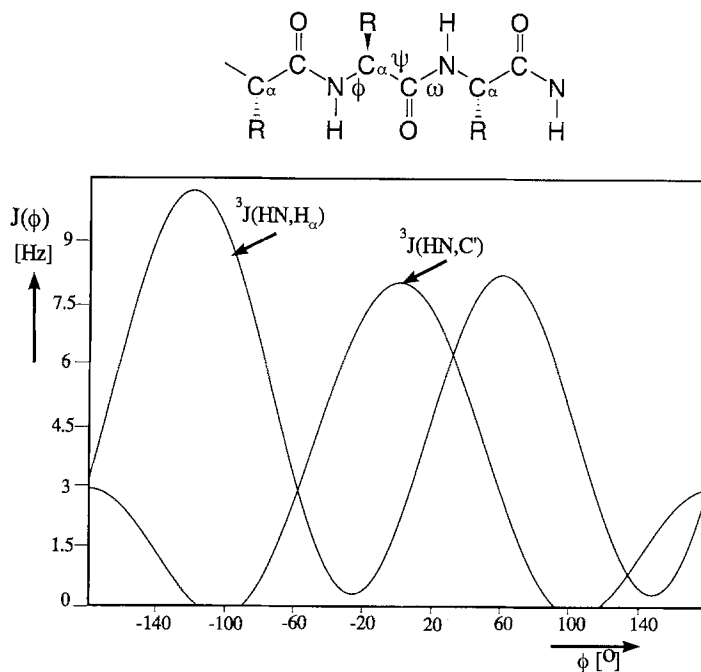
236

Fig. 3. Karplus curves for the $^3J(HN,C')$ and $^3J(HN,H_\alpha)$ coupling constants. The following Karplus parametrizations have been used (Wüthrich, 1986 and Bystrov, 1976, respectively): $^3J(HN,H_\alpha) = 6.4\ cos^2(\phi - 60) - 1.4\ cos(\phi - 60) + 1.9$; $^3J(HN,C') = 5.8\ cos^2(\phi - 60) - 2.7\ cos(\phi - 60) + 0.1\ sin^2(\phi - 60)$.

$2N^\pm(H^N)_z(H_\alpha)^\alpha$ and $2N^\pm(H^N)_z(H_\alpha)^\beta$. The following parameters were assumed: $^3J(H^N,H_\alpha)$ from 0.0 to 9.0 Hz (step size 0.1 Hz), $^3J(H_\alpha,H_\beta)$ as 12 and 3 Hz, and $^3J(N,H_\beta)$ as −1 and −4.5 Hz. A fixed $^2J(N,H_\alpha)$ of 5 Hz was assumed. The resulting intensity of the undesired coherence transfer between nonconnected transitions (e.g., from H_α in the β-state to H_α in the α-state) is less than 5% of the transfer between connected transitions. Therefore, the systematic errors introduced by the evolution of homonuclear couplings in the N→H^N transfer step can safely be neglected in the following.

However, a frequency-dependent phase is introduced due to the evolution of $^3J(H^N,H_\alpha)$ during 2ε. This phase difference Δϕ between the upper and lower trace of the E.COSY multiplet is given by

$$\Delta\phi = {}^3J(H^N,H_\alpha) \cdot 360° \cdot 2\varepsilon$$

and can take significant values (18°, assuming a coupling of 10 Hz and a delay 2ε of 5 ms). This effect would lead to an overestimation of the coupling and is compensated for in the fitting procedure of the coupling (see below).

Aliphatic selective 180° and 90° carbon pulses were implemented by G3 and G4 Gaussian cascades (Emsley and Bodenhausen 1989, 1990) of 256 and 409.6 μs duration, respectively. The selective 180° pulse on C' was implemented as phase-modulated G3 pulse of 409.6 μs. Aliphatic as well as carbonyl carbons are simultaneously decoupled during detection using double phase-
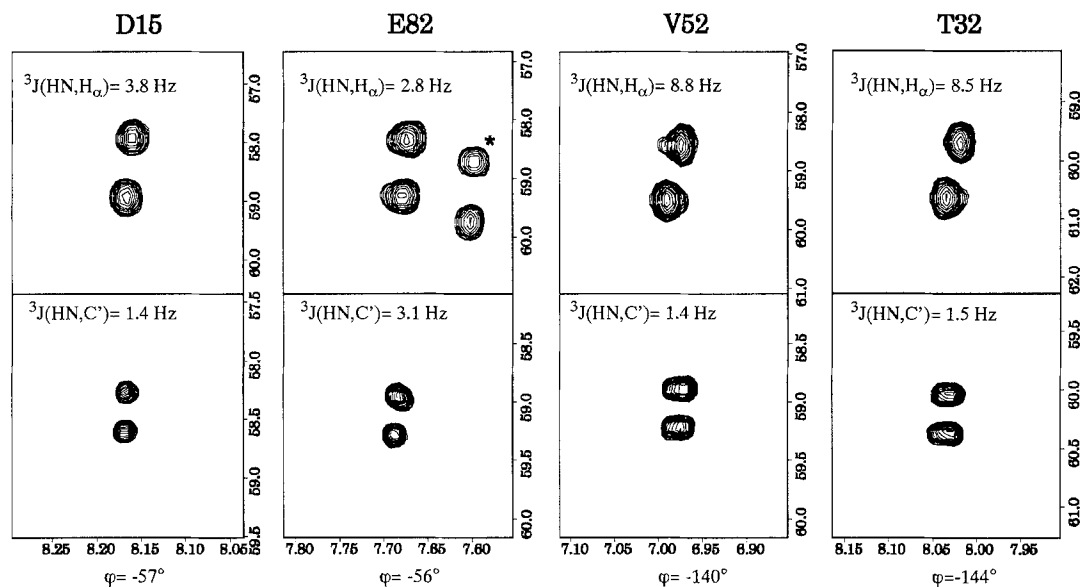
Fig. 4. Two-dimensional plots for D15, T32, V52 and E82. In the upper row, the ω_2,ω_3-slices from the HNCA-COSY are shown, in the lower row the corresponding slices from the HNCA-E.COSY. The determined coupling constants as well as the derived ϕ-angles are indicated. The multiplet marked with an asterisk appears only in the Soft HNCA-COSY and is found in a neighbouring slice of the Soft HNCA-E.COSY due to a slightly different offset. The spectra were processed using the programs UXNMR and FELIX, with the usual cosine-squared apodization in all three dimensions. The matrix of the HNCA-COSY spectrum consisted of $1024 \cdot 256 \cdot 64$ real points in $\omega_3,\omega_2,\omega_1$, with a digital resolution of 4.4, 19.5 and 31.6 Hz, respectively. The matrix of the Soft HNCA-E.COSY consisted of $512 \cdot 512 \cdot 64$ real points. In order to achieve the same digital resolution as in the HNCA-COSY experiment, the latter experiment was strip-transformed in ω_3.

modulated G3-MLEV-16 decoupling (Eggenberger et al. (1992b); for selective decoupling see also Zuiderweg and Fesik (1991) and McCoy and Müller (1993)).

Measurement of $^3J(H^N,C')$: Soft HNCA-COSY or gradient sensitivity-enhanced Soft HNCA-COSY

The experiment (Fig. 2B) for the measurement of $^3J(H^N,C')$ is again derived from the HNCA experiment, this time leaving C' passive. In principle, this experiment can be implemented as a gradient and a non-gradient version. The sensitivity-enhanced $C^{(aliphatic)}$ selective 3D CT-HNCA-COSY employs constant time evolution of the ^{15}N chemical shift during t_1 and of the ^{13}C chemical shift during t_2. Sensitivity enhancement in conjunction with a heteronuclear gradient echo is employed as in the Soft HNCA-E.COSY experiment. The protons are decoupled after appropriate defocussing and refocussing periods throughout the sequence, using DIPSI-2 decoupling (Shaka et al., 1988). In t_3, aliphatic carbons are selectively decoupled using G3-MLEV-16. The constant time delay for the C_α evolution is set to $1/{}^1J(C_\alpha,C_\beta)$, in order to decouple the aliphatic carbon–carbon couplings of around 37 Hz and to resolve the passive $^1J(C_\alpha,C')$ coupling in ω_1. Since protons can be decoupled through the major part of the experiment, the sensitivity losses in the carbon evolution period compared to the experiment without constant time evolution are acceptable. In our hands, however, the experiments with gradient coherence selection did not

TABLE 1
$^3J(H^N,C')$ AND $^3J(H^N,H_\alpha)$ COUPLING CONSTANTS AS DETERMINED WITH SOFT HNCA-COSY, SOFT HNCA-E.COSY AND GRADIENT SOFT HNCA-E.COSY EXPERIMENTS AND CORRESPONDING φ-ANGLES[a]

Residue	$^3J(N^H,H_\alpha)$	$^3J(N^H,C')$	$^3J(N^H,H_\alpha)$ grad. enh.	φ (X-ray)	φ $^3J(N^H,H_\alpha)$	φ $^3J(N^H,C')$
D15	3.8 ± 0.2	1.4 ± 0.2	4.1 ± 0.2	−59	**−56 − −58** 10 − 14 106 − 110 175 − 178	71 − 75 **−71 − −75** 137 − 143 −137 − −143
A21	3.6 ± 0.3	2.2 ± 0.2	4.1 ± 0.4	−61	**−52 − −57** 6 − 13 107 − 113 171 − 177	64 − 67 **−64 − −67** 149 − 156 −149 − −156
T32	8.5 ± 0.3	1.5 ± 0.4	8.2 ± 0.2	−141	**−140 − −147** −90 − −96	**−135 − −145** 135 − 147 65 − 75 −65 − −75
S37	5.5 ± 0.2	2.6 ± 0.2	5.0 ± 0.3	+40	**−68 − −72** −168 − −171 28 − 33 87 − 92	**−60 − −64** 60 − 64 156 − 165 −156 − −165
F48	4.6 ± 0.4	0.5 ± 0.2	4.5 ± 0.3	−64	**−60 − −67** 16 − 24 95 − 104	**−80 − −86** 80 − 86 123 − 129 −123 − −129
V52	8.8 ± 0.2	1.4 ± 0.3	8.2 ± 0.2	−114	**−138 − −143** −96 − −101	**−136 − −145** 136 − 145 70 − 77 −70 − −77
D76	7.7 ± 0.3	0.0 ± 0.2	overlap	−104	**−85 − −91** −149 − −154	**−88 − −100** 88 − 100 107 − 121 −107 − −121
E82	2.8 ± 0.2	3.1 ± 0.2	2.5 ± 0.2	−60	**−43 − −48** −3 − 3 117 − 123	**−56 − −60** 56 − 60
N84	5.8 ± 0.2	1.8 ± 0.3	5.7	+61	**−71 − −74** 31 − 37 −165 − −169 83 − 88	**−68 − −72** 68 − 72 142 − 151 −142 − −151
F100	7.3 ± 0.2	0.3 ± 0.2	overlap	−135	**−83 − −86** −154 − −157	**−83 − −90** 83 − 90 118 − 126 −118 − −126

[a] The φ-angles in column 4 are taken from an X-ray analysis (Martinez-Oyanedel et al., 1991); those in column 5 are taken from the analysis of the coupling constants determined in the two non-gradient experiments. The resulting φ-angle is given in bold. φ-angles are given in degrees and coupling constants in Hz.

show the same multiplet splitting as the non-gradient version of the experiments, the reason for which is under current investigation.

RESULTS AND DISCUSSION

The sequences of Fig. 2 have been applied to a uniformly $^{13}C,^{15}N$-labeled sample of ribonuclease T_1 in H_2O. Figure 3 shows Karplus curves for the couplings of interest. Figure 4 shows four representative cross peaks from the HNCA-COSY and HNCA-E.COSY spectra for residues with, according to the X-ray structure, different ϕ-angles (Martinez-Oyanedel et al., 1991). Table 1 lists the derived coupling constants for a number of different residues, together with the ϕ-angle derived from the X-ray structure and from the analyses of the two experiments.

For D15, A21, T32, F48, D76 and E82, the resulting ϕ-angle of the combined analysis of the two experiments is in good agreement with the angle derived from the X-ray structure analysis. For E82 the $^3J(H^N,H_\alpha)$ coupling is fulfilled for four different ϕ-angles. The measurement of the additional $^3J(H^N,C')$ leads unambiguously to a ϕ-angle of $-56°$. The ϕ-angle of V52 in solution differs from the angle in the crystal structure by $30°$. N84 and S37 are the only non-glycine residues in the X-ray structure of ribonuclease T_1 with a positive ϕ-angle. The analysis of the coupling constants for both residues suggests that the ϕ-angles in solution are around $-70°$, a value more commonly found in proteins, rather then $+61°$ and $+40°$, as found in the X-ray structure for N84 and S37. A distance geometry calculation using ϕ-angle constraints derived from these experiments, in combination with NOE distance constraints, is currently in progress.

The values of the coupling constants and their rms deviations have been determined by taking appropriate ω_3 traces, displacing them with respect to each other by J^{trial} and forming the integral of the power difference spectrum P as a function of the displacement: $P(J^{trial})$. The coupling constant J_0 is determined at the minimum of the integral, i.e., $P(J_0) = min$. The statistical error of the power difference integral is determined by varying the integration region in ω_3, rms $(P(J^{trial}))$, thus introducing the effects of random noise. The statistical error is determined from the error of the integral power difference by parabolic extrapolation of $P(J^{trial})$ about J_0 (Schwalbe et al., 1993).

CONCLUSIONS

In conclusion, we have introduced sensitive methods for quantitative measurements of H^N,H_α and H^N,C' coupling constants in uniformly $^{13}C,^{15}N$-labeled proteins. Measuring these two coupling constants allows the unambiguous determination of the ϕ-angle in proteins and will further improve the quality of NMR structure determinations.

NOTE ADDED IN PROOF

Similar work has been performed independently by Stephan Seip, Jochen Balbach and Horst Kessler, TU München, Germany.

ACKNOWLEDGEMENTS

REFERENCES

Cavanagh, J., Palmer III, A.G., Wright, P.E. and Rance, M. (1991) *J. Magn. Reson.*, **93**, 151–170.
Eggenberger, U., Karimi-Nejad, Y., Thüring, H., Rüterjans, H. and Griesinger, C. (1992a) *J. Biomol. NMR*, **2**, 583–590.
Eggenberger, U., Schmidt, P., Sattler, M., Glaser, S.J. and Griesinger, C. (1992b) *J. Magn. Reson.*, **100**, 604–610.
Emsley, L. and Bodenhausen, G. (1989) *J. Magn. Reson.*, **82**, 211–221.
Emsley, L. and Bodenhausen, G. (1990) *Chem. Phys. Lett.*, **65**, 469–476.
Farmer, II, B.T., Venters, R.A., Spicer, L.D., Wittekind, M.G. and Müller, L. (1992) *J. Biomol. NMR*, **2**, 195–202.
Griesinger, C., Sørensen, O.W. and Ernst, R.R. (1985) *J. Am. Chem. Soc.*, **107**, 6394–6396.
Griesinger, C., Sørensen, O.W. and Ernst, R.R. (1986) *J. Chem. Phys.*, **85**, 6837–6852.
Griesinger, C., Sørensen, O.W. and Ernst, R.R. (1987) *J. Magn. Reson.*, **75**, 474–492.
Grzesiek, S. and Bax, A. (1990) *J. Magn. Reson.*, **89**, 432–440.
Ikura, M., Kay, L.E. and Bax, A. (1990) *Biochemistry*, **29**, 4659–4668.
Kay, L.E., Ikura, M. and Tschudin, R. and Bax, A. (1990) *J. Magn. Reson.*, **89**, 496–514.
Kay, L.E., Keifer, P. and Saarinen, T. (1992) *J. Am. Chem. Soc.*, **114**, 10663–10665.
Levitt, M.H., Freeman, R. and Frenkiel, T. (1982) *J. Magn. Reson.*, **47**, 308–320.
Madsen, J.C., Sørensen, O.W., Sørensen, P. and Poulsen, F.M. (1993) *J. Biomol. NMR*, **3**, 239–244.
Martinez-Oyanedel, J., Choe, H.-W., Heinemann, U. and Sänger, W. (1991) *J. Mol. Biol.*, **222**, 335–346.
McCoy, M.A. and Müller, L. (1993) *J. Magn. Reson. Ser. A*, **101**, 122–130.
Messerle, B.A., Wider, G., Otting, G., Weber, C. and Wüthrich, K. (1989) *J. Magn. Reson.*, **85**, 608–613.
Muhandiram, D.R., Guang, Y.X. and Kay, L.E. (1993) *J. Biomol. NMR*, **3**, 463–470.
Palmer III, A.G., Cavanagh, J., Wright, P.E. and Rance, M. (1991) *J. Magn. Reson.*, **91**, 429–436.
Schleucher, J., Sattler, M. and Griesinger, C. (1993) *Angew. Chem.*, **105**, 1518–1521; (1993) *Angew. Chem., Int. Ed. Engl.*, **32**, 1489–1491.
Schwalbe, H., Rexroth, A., Eggenberger, U., Geppert, T. and Griesinger, C. (1993) *J. Am. Chem. Soc.*, **115**, 7878–7879.
Seip, S., Balbach, J. and Kessler, H. (1992) *Angew. Chem.*, **104**, 1656–1658.
Shaka, A.J., Lee, C.J. and Pines, A. (1988) *J. Magn. Reson.*, **77**, 274–293.
Shaka, A.J., Barker, P.B. and Freeman, R. (1985) *J. Magn. Reson.*, **64**, 547–552.
Sørensen, O.W. (1984) Ph.D. Thesis, ETH-Zentrum, Zürich.
Sørensen, O.W. (1990) *J. Magn. Reson.*, **90**, 433–438.
States, D.J., Haberkorn, R.H. and Ruben, D.J. (1982) *J. Magn. Reson.*, **48**, 286–292.
Vuister, G. and Bax, A. (1992) *J. Biomol. NMR*, **2**, 401–405.
Wagner, G., Schmieder, P. and Thanabal, V. (1991) *J. Magn. Reson.*, **93**, 436–440.
Wüthrich, K. (1986) *NMR of Proteins and Nucleic Acids*, Wiley, New York, NY, p. 167.
Zuiderweg, E.R.P. and Fesik, S.L. (1991) *J. Magn. Reson.*, **93**, 653–658.